Taylor & Francis
Taylor & Francis Group

Artificial Cells, Nanomedicine, and Biotechnology

An International Journal

ISSN: 2169-1401 (Print) 2169-141X (Online) Journal homepage: informahealthcare.com/journals/ianb20

Aligned bacterial PHBV nanofibrous conduit for peripheral nerve regeneration

Murat Demirbilek, Mustafa Sakar, Zeynep Karahaliloğlu, Ebru Erdal, Eda Yalçın, Gökhan Bozkurt, Petek Korkusuz, Elif Bilgiç, Çağrı Mesut Temuçin & Emir Baki Denkbaş

To cite this article: Murat Demirbilek, Mustafa Sakar, Zeynep Karahaliloğlu, Ebru Erdal, Eda Yalçın, Gökhan Bozkurt, Petek Korkusuz, Elif Bilgiç, Çağrı Mesut Temuçin & Emir Baki Denkbaş (2015) Aligned bacterial PHBV nanofibrous conduit for peripheral nerve regeneration, Artificial Cells, Nanomedicine, and Biotechnology, 43:4, 243-251, DOI: 10.3109/21691401.2013.875033

To link to this article: https://doi.org/10.3109/21691401.2013.875033

Artificial Cells, Nanomedicine, and Biotechnology, 2015; 43: 243–251

ISSN: 2169-1401 print / 2169-141X online
DOI: 10.3109/21691401.2013.875033

Taylor & Francis
Taylor & Francis Group

Aligned bacterial PHBV nanofibrous conduit for peripheral nerve regeneration

Murat Demirbilek[1], Mustafa Sakar[2], Zeynep Karahaliloğlu[3,4], Ebru Erdal[3,4], Eda Yalçın[3], Gökhan Bozkurt[2], Petek Korkusuz[5], Elif Bilgiç[5], Çağrı Mesut Temuçin[6] & Emir Baki Denkbaş[7]

[1]*Bayındır Hospital, Söğütözü, Ankara, Turkey,* [2]*Department of Neurosurgery, Hacettepe University Faculty of Medicine, Sıhhiye, Ankara, Turkey,* [3]*Division of Nanotechnology and Nanomedicine, Department of Chemistry, Hacettepe University, Beytepe, Ankara, Turkey,* [4]*Department of Biology, Aksaray University, Aksaray, Turkey,* [5]*Department of Histology and Embryology, Hacettepe University Faculties of Medicine, Sıhhiye, Ankara, Turkey,* [6]*Department of Neurology, Hacettepe University Faculty of Medicine, Sıhhiye, Ankara, Turkey, and* [7]*Division of Biochemistry, Department of Chemistry, Hacettepe University, Beytepe, Ankara, Turkey*

Abstract

The conventional method of peripheral nerve gap treatment is autografting. This method is limited. In this study, an aligned nanofibrous graft was formed using microbial polyester, Poly (3-hydroxybutyrate-co-3-hydroxyvalerate) (PHBV). The regenerative effect of the graft was compared with that of autografting *in vivo*. To determine the regenerative effect, rats were assessed with sciatic nerve functional index, electromyographic evaluation, and histological evaluation. Results found in this study include PHBV grafts stimulated progressive nerve regeneration, although regeneration was not comparable with that of autografting. We conclude that the study results were promising for aligned bacterial polymeric grafts for peripheral nerve regeneration.

Keywords: aligned scaffold, bacterial PHBV, peripheral nerve regeneration, regenerative medicine

Introduction

Peripheral nerve injury has serious socioeconomic effects, since it results with loss of sensation, motor weakness, and painful neuropathies (Noble et al. 1998). A key for peripheral nerve injury repair is their ability of regeneration. Axons within the peripheral nerve are capable of regenerating across the lesion site and form functional connections. The gold standard for peripheral nerve injury is simple suturing of the damaged nerve ends or, if there is a gap that cannot be sutured; a nerve autograft is used (Yu and Bellamkonda 2003). However, many disadvantages of autografting include limited donor nerve sources, potential loss of function at donor sites, and the requirement of multiple surgeries. Allografting and xenografting are hampered by immunological rejections (Trumble and Shon 2000). Because of these disadvantages, an alternative approach, tissue-engineered scaffolds, may serve as an option for neural tissue engineering. The physical and chemical properties of polymeric grafts can be tailored based on applications. Polymeric scaffolds may provide tissue regeneration, by controlling scaffold morphology, architecture and components, and topographical and biochemical properties (Jain et al. 2006). Therefore, bioengineering strategies attempt to mimic the nerve autografts and aim to develop nerve conduits. To replace the nerve autografting, nerve conduits must be biocompatible and degradable materials. They must also lead the axons to cross the lesion site and reinnervate the appropriate target for functional recovery.

Many natural and synthetic materials have been used to produce a nerve conduit in the literature including polyethylene (Stevenson et al. 1994), silicon and collagen (Chamberlain et al. 1998), poly tetrafluoroethylene (Valentini et al. 1989), collagen and polyglycolide (Kiyotani et al. 1995), and silicon (Chen et al. 2001). However, both natural and synthetic materials can cause an immune response from degradation products, chemical leaching such as monomer or initiator. Also elasticity of the graft may affect the biocompatibility, depending on the mechanical properties.

Poly (3-hydroxybutyrate-co-3-hydroxyvalerate) (PHBV) is a member of Polyhydroxyalkanoates (PHAs) family. It is a copolymer consists of 3-hydroxybutyrate (3HB) and 3-hydroxyvalerate (3HV). PHAs are produced by a number of bacteria, such as *Alcaligenes eutrophus,* under nutrient depletion conditions as intracellular storage material of carbon and energy. For bacteria culture, sugars such as sucrose and glucose are the most common main carbon sources and propionic acid or valeric acid are usually added to the medium for copolymer production (Anil Kumar et al.

Correspondence: Emir Baki Denkbaş, Division of Biochemistry, Department of Chemistry, Hacettepe University, Beytepe, Ankara 06800, Turkey. E-mail: denkbas@hacettepe.edu.tr

(Received 3 October 2013; accepted 3 December 2013)

2007). PHAs are used in many tissue engineering studies in the literature including sutures, adhesion barriers, and they guide tissue repair/regeneration devices, articular cartilage repair devices, tendon repair devices, bone-marrow scaffolds, wound dressing (Baki 2010), and cardiovascular patches (Gaudio et al. 2012).

In this study, bacterial PHBV was produced by *A. eutrophus* using propionic acid. Electrospinning technique was the method for preparing the scaffold. The scaffold was shaped into a tube to use as a nerve graft. Sciatic nerve gaps which were formed just before the procedure experimentally were repaired using this conduit. After implantations, functional and histological tests were performed and obtained results were compared with autografting. In this study, we aimed to investigate the nerve regeneration potential of PHBV grafts, and to compare the results with autografting, which is still the gold standard for peripheral nerve injury today.

Materials and methods

Materials

A. eutrophus was obtained from Biology department of Osmangazi University, Eskişehir, Turkey. All aqueous chemicals were obtained from Sigma-Aldrich, USA. The electrospinning apparatus comprised of a high-voltage power supply, 0–30kV (A CZE1000R Spellman, USA), a syringe pump (Biasis, Turkey), a cylindrical aluminum drum collector with 35 mm in diameter, and 3100 rpm were used.

Bacterial PHBV production

A. eutrophus (DSM 545) was used for PHBV production. Production procedures were adapted from the related literature (Yoon et al. 1997). Briefly, two-step cultivation was performed with pre-culture and polymer medium. The precultured medium was containing 10 g/L glucose, 2 g/L yeast extract, 2 g/L peptone, 1 g/L K_2HPO_4, 1 g/L KH_2PO_4, 1 g/L NH_4 SO4, and 0.05 g/L $MgSO_4.7H_2O$ (pH = 7). The polymer medium was containing 10 g/L glucose, 0.83 g/L KH_2PO_4, 3 g/L NH_4Cl, 1.33 g/L $Na_2HPO_42H_2O$, 2 g/L $NaHCO_3$, 20 g/L propionic acid, 2 g/L $MgSO_4.7H_2O$, and 300µg/L trace elements (pH = 7). Trace element solution was consisted of 0.218 g $CoC1_2$. $6H_20$, 16.2g $FeC1_3.6H_20$, 10.3 g $CaC1_2.2H_20$, 0.118 g $NiC1_2.6H_20$, 0.133g $CrCl_3.6H_2O$, 0.1 g $CuS0_4$, and 15.6 g citric acid in 100 mg 1 N HCl.

The bacteria were cultivated at 32°C for 24 h in preculture medium and harvested by centrifugation at 5000 rpm for 15 min., then cultured in polymer medium. The cultivation condition was at 32°C and 150 rpm for 2 days. PHBV was purified and characterized by H-NMR (Bruker model AC400) (Susheela 2012).

Aligned nanofiber bacterial PHBV scaffold preparation

The nanofibrillar scaffolds were prepared using electrospinning technique. Five percent (w/v) PHBV solution was prepared in chloroform at 60°C. The polymer solution was then delivered to a 20-gauge metal needle (OD = 0.91mm) connected to a high-voltage power supply. A high-voltage power supply was used to generate a fixed potential of 20kV. The polymer solutions were delivered at 2 ml/h flow rate using Goldman syringe pump. The distance between the tip of the syringe and collector was 15 cm. A drum collector at 3100 rpm was used in the study (Zhao et al. 2008).

The morphological appearance of the nanofibrillar scaffolds was observed using scanning electron microscope (ZEISS EVO 50 EP, Germany) (Chew et al. 2007).

The tensile properties of the aligned scaffolds were measured at room conditions using a 100 N load cell on Zwick/Z010 tensile tester. The extension was set at 10 mm/min. Six scaffolds were tested and the average results with standard deviation were presented (Koh et al. 2008).

Surgery and PHBV graft implantation

Aligned PHBV nanoscaffold was shaped into a tube. Internal diameter of the tube was 1 mm, the wall thickness was approximately 0.75 mm and length of the tube was 15mm. In animal experiment, rats were randomly assigned to two groups as autograft and PHBV graft groups. Group 1 animals, autograft group, ($n = 9$), were used as control. In Group 2 ($n = 27$), biodegradable bacterial PHBV tubes were used as nerve conduits to repair the 10-mm defect formed in right rat sciatic nerves experimentally. Thirty-six female Sprague-Dawley rats, weighing 200–250 gr were provided by Hacettepe University Animal Laboratory, Ankara, Turkey and all procedures involving animals were approved by the Animals Committee of the Hacettepe University. All operative procedures were performed under aseptic conditions using Zeiss surgical microscope (Carl Zeiss AG, Jena, Germany). The animals were anesthetized by intraperitoneal injection of ketamine hydrochloride (100 mg/kg) and xylazine (5 mg/kg). Under intraperitoneal anesthesia, right sciatic nerve of each animal was exposed and 10-mm nerve gap was formed. In Group 1 animals (autologous graft, $n = 9$), the right sciatic nerve defect was repaired with the excised reverse oriented sciatic nerve using 10-0 nylon sutures (Ethicon). In PHBV graft group ($n = 27$), the nerve defects were repaired with a PHBV tube. 2.5-mm long nerve was placed into the PHBV tube at proximal and distal stumps. The tube was attached to the proximal and distal nerve stumps using the 10-0 nylon sutures (Ethicon). The tubes were placed in the sciatic nerve gaps so that the alignment of the nanofibers in the inner surface of the graft may provide axonal regeneration. The tubes were filled with a drop of 1% agarose to prevent a collapse. After hemostasis the skin incisions were closed with surgical staples in both groups. Rats were housed, fed routinely, and monitored for changes in their ordinary conditions and motor activities.

Electrophysiological assessment

Four and sixteen weeks after the surgery, electrophysiological assessment was performed as a functional test for evaluation of the axonal regeneration. Rats were anesthetized with ketamine (100 mg/kg), fixed with tape on a smooth table, and heated to avoid hypothermia. An active needle electrode was inserted on the belly of the gastrocnemius muscle in the middle of the paw, while the reference needle electrode was placed subcutaneously between the

first and second digit. The right (operated) and left (control) sciatic nerves were stimulated at the level of sciatic notch, proximal to the nerve gap, and compound motor action potentials (CMAP) were recorded. The negative peak amplitude (mV) of CMAP of sciatic nerves was calculated. Normal CMAP amplitudes were obtained from the contralateral non-operated side (Mligiliche et al. 2001).

The recovery index was calculated based on the following formula:

$$\text{Recovery index (CMAP\%)} = \frac{\text{Negative peak amplitude of operated side}}{\text{Negative peak amplitude of control side}} \times 100$$

Walking analysis

Walking analysis was also performed to assess motor functional recovery. Thus, sciatic functional index (SFI), described in the literature was employed as a functional test. Two, 4 and 16 weeks after nerve repair, walking tests were performed. For walking test, a glass box (10-cm deep, 10-cm width, and 100-cm long) was used. Rat toes were stained with methylene blue and rats were leaded to walk on a soft paper to obtain toe prints (Ozkan et al. 2010).

SFI values were calculated on the following formulas:

$$\text{Print length factor (PLF)} = \frac{(\text{Experimental PL} - \text{Normal PL})}{\text{Normal PL}}$$

$$\text{Toe spread factor (TSF)} = \frac{(\text{Experimental TS} - \text{Normal TS})}{\text{Normal TS}}$$

$$\text{Intermediary toe spread factor (ITF)} = \frac{(\text{Experimental IT} - \text{Normal IT})}{\text{Normal IT}}$$

$$\text{SFI} = -38.3 \times \text{PLF} + 109.5 \times \text{TSF} + 13.3 \times \text{ITF} - 8.8$$

Histological assessment

Histological assessment was used to determine the number of regenerated axons and the thickness of new myelin. After scarification, rats were intracardially perfused with 2% paraformaldehyde in 0.1 mol/L cacodylate buffer at pH 7.4 and 2% glutaraldehyde in 0.1 mol/L cacodylate buffer at pH 7.4 until the lower extremities are fixed. The peripheral nerve was carefully dissected and fixed by immersion in 2.5% glutaraldehyde in cacodylate buffer. Rinsed in buffer and, post-fixed in 1% osmium tetroxide in cacodylate buffer at 4°C for 2 h. Specimens were dehydrated in graded series of ethanol to absolute ethanol in preparation for embedding in epon (EMS, Germany) using an automated tissue processor (Leica, Wetzlar, Germany).

Semi-thin sections were stained with methylene blue-azur II (a minimum of 10 sections obtained from different levels of each tissue) and examined with a Leica DMR microscope (Germany). The images were captured via Leica DC500 digital camera (Wetzlar, Germany) and quantitatively evaluated using Leica application suite and Qwin software for the morphologic peripheral nerve regeneration criteria modified from the literature (Chun et al. 2007). The whole image of the histological cross-section was digitized and subsequently analyzed for its total surface area. The total number of axons and the blood vessels were separately counted in this area. The axon and blood vessel numbers were then extrapolated by applying the area algorithm to estimate the total number of axons for each nerve. The tissue response to the biomaterial was semi-quantitatively scored for the biomaterial-applied groups according to the literature related to the soft-tissue implants (Bolgen et al. 2007).

Thin sections were stained with uranyl acetate and lead citrate with an automated staining machine (Leica, Germany), analyzed on a transmission electron microscope (Jeol, JEM1400) attached Orius digital camera for ultra-structure myelin sheath regeneration criteria. Thickness of the myelin sheath was measured in micrometer for at least 10 axons on at least three ultra-sections belonging to each sample (Dodla and Bellamkonda 2008).

Data analysis and statistics

Independent variables were the groups and the dependent variables were the histology and functional analysis parameters. The normality of distribution and the homogeneity of variances of the sample were established using the Shapiro–Wilk test. All parameters were analyzed by nonparametric tests. Kruskal–Wallis was used for multiple comparison and Mann–Whitney U as post-hoc test with Bonferroni correction. Descriptive statistical values were expressed as median, minimum, and maximum. Statistical significance was determined using SPSS software (version 15.0). The differences were considered significant when $p < 0.05$.

Results

Bacterial PHBV production and characterization

Structural analysis of the PHBV was performed by H-NMR (Figure 1). The standard peaks were obtained at 0.80–0.90 (-CH_3 of Hydroxyvalerate), 1.20–1.35 (-CH_3 of Hydroxybutirate), 2.20–2.70 (-CH_2 of Hydroxybutirate and Hydroxyvalerate), and 5.4–5.8 (–CH of Hydroxybutirate and Hydroxyvalerate) (Jian et al. 2009).

Aligned nanofiber bacterial PHBV scaffold preparation and characterization

Electrospinning parameters were optimized during this study to obtain bead-free, uniform, and aligned nanofibers. Figure 2 reveals the SEM micrographs showing the morphology of electrospun PHBV nanofibrous scaffolds. PHBV nanofibers with average diameters of 400–600 nm were obtained.

Tensile strength, elongation at break and E modulus values of PHBV nanofiber scaffolds ($n = 6$) were determined and mechanical test results showed that aligned PHBV nanofiber scaffold has proper mechanical properties. The mean value and standard deviation found for tensile strength (N/mm^2) was 18.33 ± 1.32; elongation at break (%) was 19.33 ± 0.4, and E modulus was 195.26 ± 13.98.

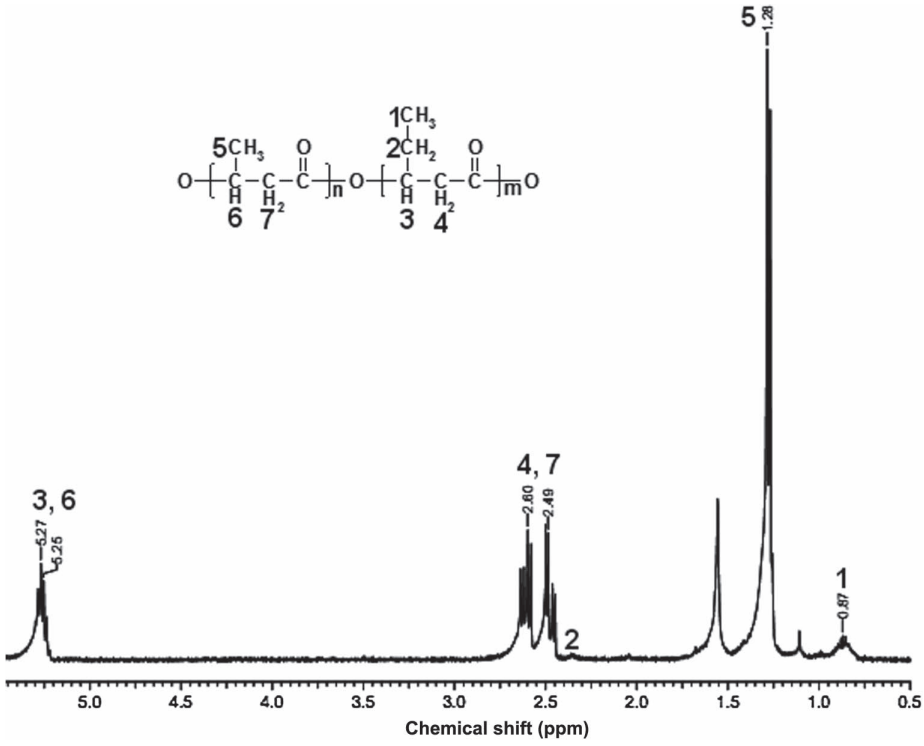

Figure 1. H-NMR spectrum of bacterial PHBV produced by using propionic acid.

Surgery and PHBV graft implantation

Aligned PHBV nanoscaffold was shaped into a tube. Internal diameter of the tube was 1 mm, the wall thickness was approximately 0.75 mm, and length of the tube was 15mm. The right sciatic nerves of 36 female Sprague-Dawley rats, weighing 200–250 gr, were used to compare PHBV nerve grafts and autograft. All animals survived in the postoperative period. Autophagy was observed for three rats and for further experiments these rats were not used. In this study no collapse was occurred (Figure 3). Muscular atrophy was observed in all rats.

Electrophysiological assessment

For evaluation of axonal regeneration, electrophysiological assessments of PHBV graft and autograft groups were performed and CMAP amplitudes (CMAP %) were calculated at seventh and sixteenth weeks after surgery (Figure 4). The results were normalized to values from the rats' not-operated leg.

At 8 weeks post-operatively, the mean CMAP amplitude (%) of autograft and PHBV graft groups were $42.18 \pm 1.84\%$, $28.94 \pm 1.29\%$, respectively. At 16 weeks post-operatively, the mean CMAP amplitude (%) of autograft and PHBV graft groups was $57.63 \pm 1.48\%$, $39.28 \pm 1.51\%$, respectively. In autograft group, mean CMAP amplitude (%) values were significantly higher than PHBV graft group both at 8th and 16th weeks. The CMAP results indicated that in PHBV graft group nerve regeneration was slower than that of autograft group at 8th and 16th weeks after operation. Also PHBV graft group did not reach similar level of muscle re-innervation as autograft group. Statistically significant differences were found between autograft and PHBV graft groups ($p < 0.05$).

Walking analysis

Rats were undergone walking analysis for assessment of nerve regeneration four, seven, and sixteen weeks after nerve repair using SFI values (Figure 5). At the 4th week, the SFI values of autograft and PHBV graft groups were 66.45 ± 7.61

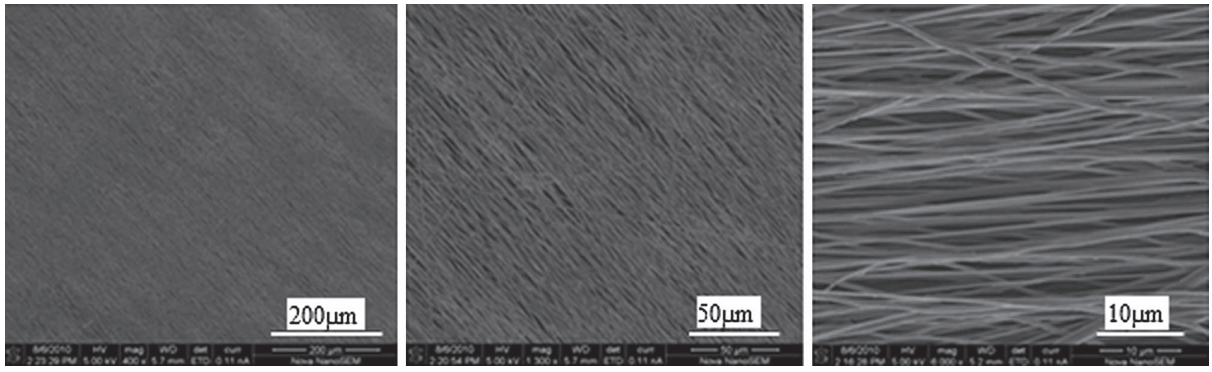

Figure 2. SEM photographs were exhibiting the alignment of the PHBV nanofiber scaffolds at different magnifications.

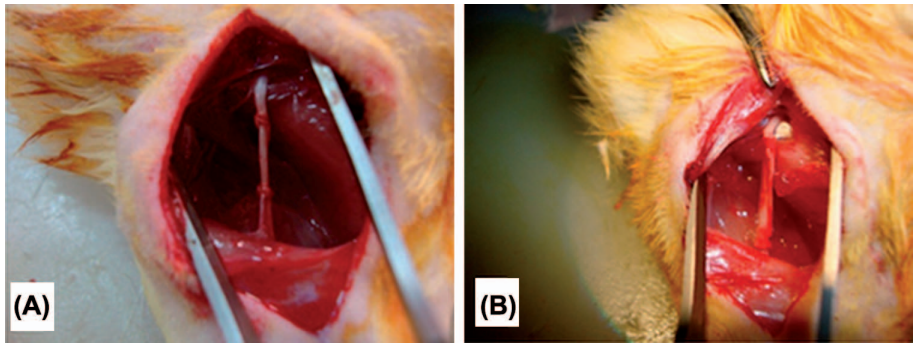

Figure 3. Surgical implantation of autograft (A) and aligned PHBV graft (B) for nerve regeneration in rat sciatic nerve under a microscope (10×).

and 75.796 ± 3.976, respectively. At the 8th week, SFI values of autograft and PHBV graft groups were 55.82 ± 1.98 and 62.92 ± 4.081, respectively. At the 16th week, SFI values of autograft and PHBV graft groups were 47.85 ± 8,130 and 55.52 ± 9.07, respectively. At the 16th week post-operatively, the mean SFI values decreased in both groups. The observed decrease on SFI values mean that some regenerated axons had passed through the nerve graft. Walking analysis showed significantly lower SFI values in the autograft group than in the PHBV group at the 4th, 8th, and 16th weeks post-operatively ($p < 0.05$). Meanwhile, at the 4th week, it was not observed statistically differences between two group ($p > 0.05$).

On the 4th postoperative week, footprints of the operated legs were longer and narrower and fingers were closer than not-operated legs in both groups. On the 8th postoperative week, footprints were slightly shorter and thicker in both groups. Finally, on the 16th week, the footprints of PHBV graft-applied legs became further shorter and thicker than not-operated legs, although less than autograft-applied legs. Footprints of the PHBV graft applied and not-operated legs are presented at Figure 6.

Histological assessment

Histological assessment was used to determine the axon number and the diameter of the myelin in the PHBV graft and autograft groups at 8th and 16th weeks after operations. PHBV graft was minimally degraded and its wall generally kept its shape in vivo and caused a moderate tissue reaction. This tissue reaction did not differ statistically between the two time periods. Both the inner and the outer surfaces of the PHBV graft exhibited a capsule consisting of mononuclear phagocytic cells, giant cells, lymphocytes, and fibroblasts making several (2–10) layers. The inner capsule was continuous with a relatively loose granulation tissue (subcapsullar tissue) rich in blood vessels crossing the nerve defect area.

In autograft group, a well-coordinated and healthy regenerating nerve exhibiting regular fascicles of axons was noted. The nerve regeneration process did not show any significant difference between 8th and 16th weeks in the autograft group. The nerve sheaths and the vascular elements were very well-defined in this group. The number of axons was significantly higher in this group when compared to those of the PHBV graft group on Week 8 ($p = 0.008$). In the PHBV graft group, the tube lumen was filled with a fibrovascular tissue containing some irregular nervous tissue elements. Some unevenly distributed baby axon groups with a rich capillary network were observed in this group. Simultaneously the PHBV graft group contained more blood vessel compared to that of the autograft group on Week 8 ($p = 0.008$). No significant difference was

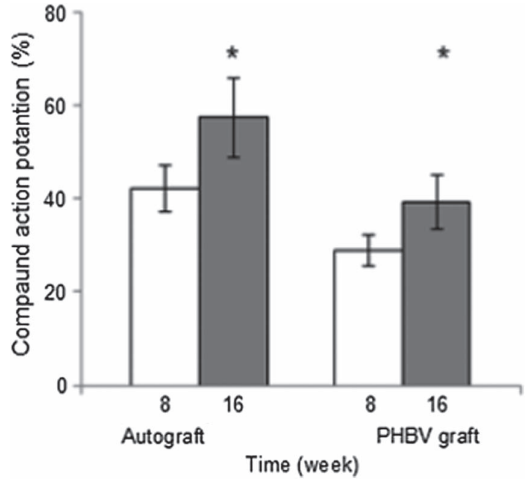

Figure 4. 8th ($n = 18$) and 16th ($n = 12$) weeks after surgery, electrophysiological assessments of autograph and PHBV graft group rats. *Statistical significance ($p < 0.05$).

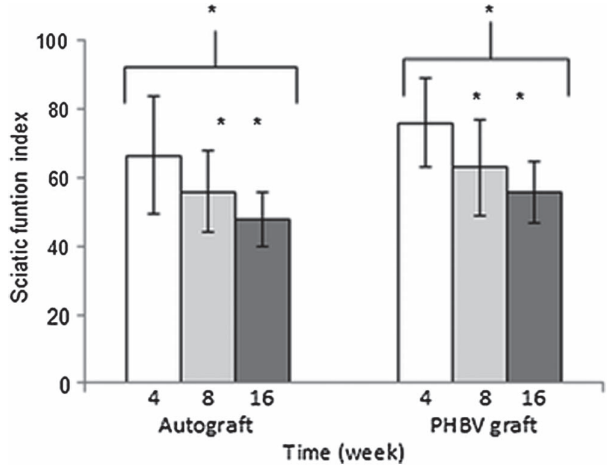

Figure 5. After 4th, 8th ($n = 18$), and 16th ($n = 12$) weeks of operations, autograft and PHBV graft group SFI values. *Statistical significance ($p < 0.05$).

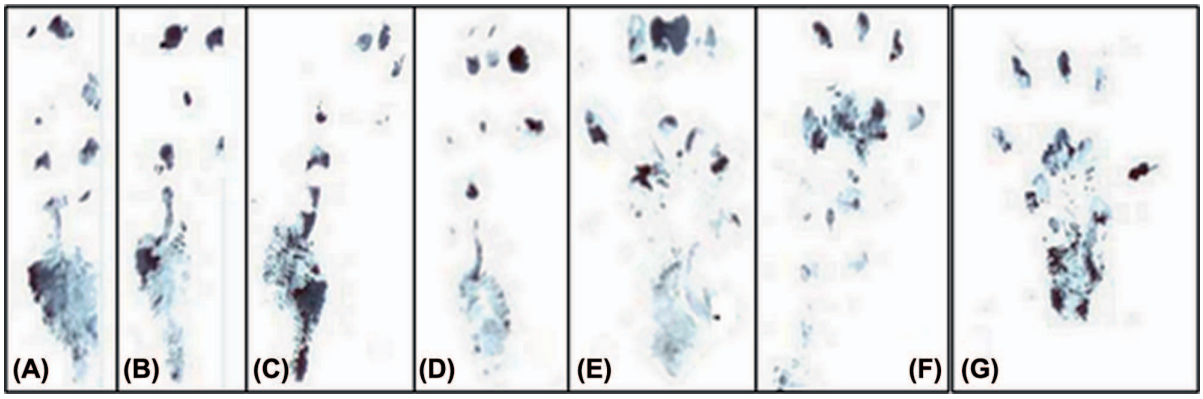

Figure 6. Footprints of PHBV graft-applied legs of the rats, after 4th (A, B); 8th (C, D); 16th (E, F) weeks and not-operated footprint (G).

observed between the PHBV graft group related to the number of the axons and the blood vessels on Week 16 (Figure 7).

At the transmission electron microscopic level, all groups exhibited varying amounts of myelinating single or clustered nerve fibers surrounded by Schwann cells. The myelin sheath thickness was not different in autograft group when compared to that of both the PHBV graft groups. As a conclusion, the PHBV graft slightly improved the nerve regeneration process compared to the control on Week 16 (Figure 8).

Discussion

We produced and tested bacterial polyester, PHBV, for potential application in peripheral nerve repair. PHAs are accumulated as intracellular polymers by a variety of microorganisms under certain nutrient limiting conditions (Longan et al. 2004). PHB is more common in PHA family but, PHBV is a more interesting polymer than PHB due to its melting point, crystal rate, and biodegradability features (Ren et al. 2000). PHBV production method was simple and includes two-step cultivation, culture medium, and

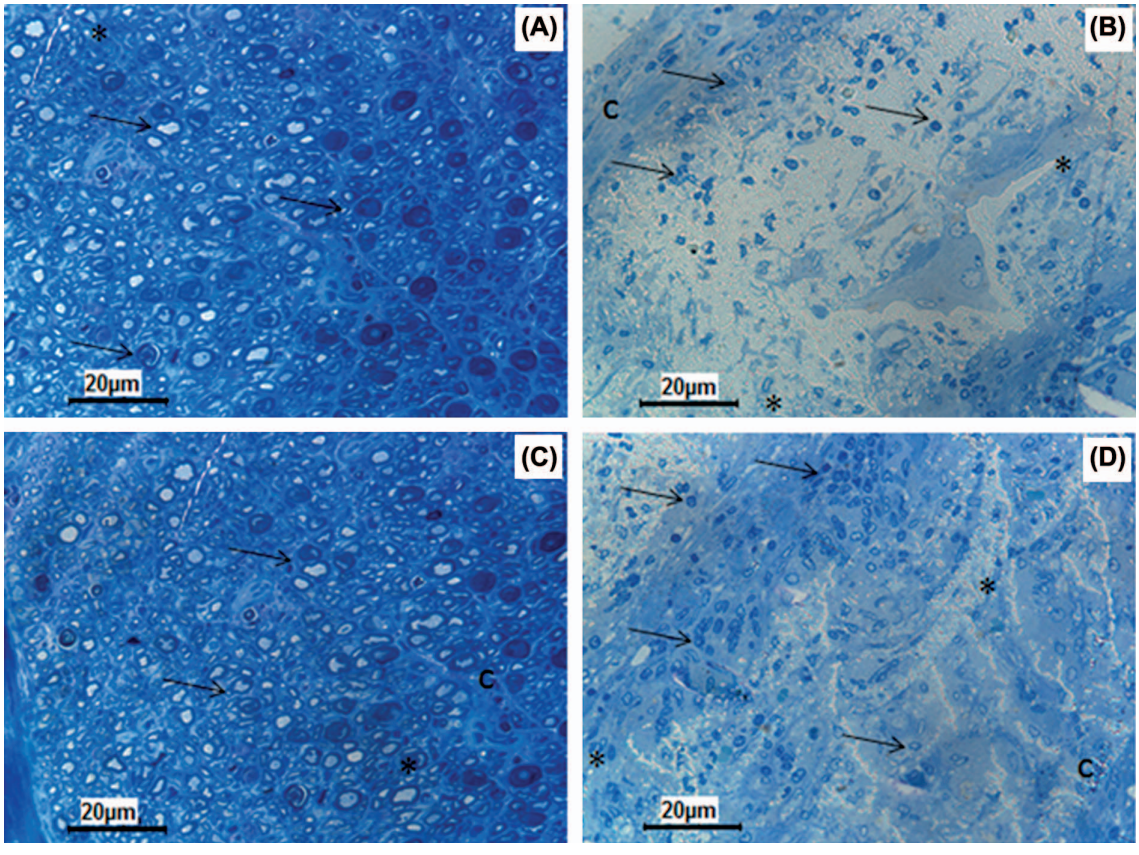

Figure 7. The regenerating numerous axons (arrow) form regular fasicles in 8th (A) and 16th (C) weeks of autograft group. The PHBV graft is surrounded by an inflammatory capsule (c) consisting of phagocytic and fibroblastic cells at its inner side at 8th week (B). In PHBV graft group at 16th week (D) the tubes lumen is filled with fibrovascular connective tissue with small blood vessels (asterisk) and regenerating axon clusters with higher numbers at the 16th week (D) compared to the 8th week (B).

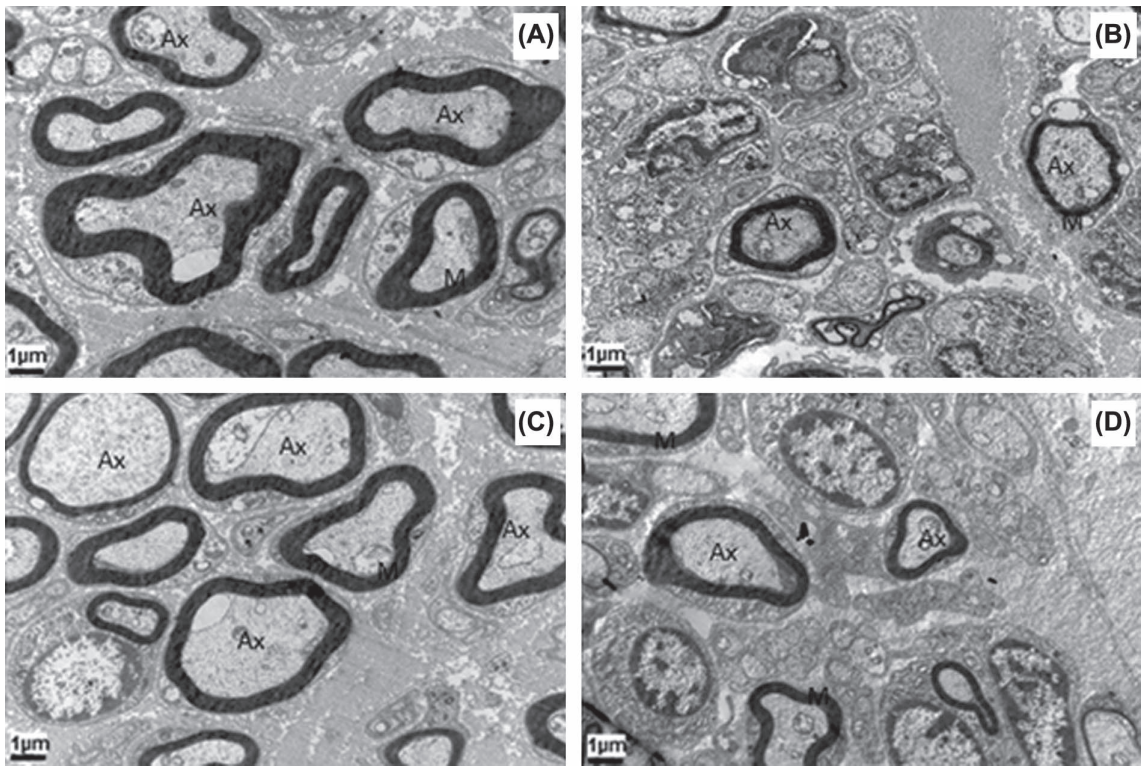

Figure 8. Transmission electron micrographs have the same magnification (12000×). All the groups show the regenerating clusters of myelinating or myelinated axons. Note that the number of axons and the thickness of their myelin sheath is higher in autograft group at the 8th (A) and 16th weeks (C) compared to PHBV graft group at the 8th (B) and 16th weeks (D). Ax: Axon; M: Myelin. Uranyl acetate and lead citrate.

polymer medium. To obtain a high concentration of PHBV, it is essential to use nitrogen-rich medium and excess carbon source. Therefore, propionic acid and also glucose were used as carbon sources in polymer medium. The cultivation temperature was 30°C and the pH was maintained at 7.0. This process was easy to scale-up for large-scale applications. In the literature, some other microorganism were used to produce PHBV including *Corynebacterium glutamicum* (Matsumoto et al. 2011) and *Rhodopseudomonas palustris* SP5212 (Mahuya et al. 2005), and several carbon sources were used for PHA production by *A. eutrophus* including lactic acid (Linko and Vaheri 1993) and acetic acid (Wang and Yu 2001).

For the characterization of the PHBV, H-NMR method was used. The NMR spectrum of the PHBV produced from *A. eutrophus* showed major peak at 1.2–1.3 corresponding to 3HB component (Figure 1). In addition a small peak at 0.8–0.9 ppm indicated the incorporation of 3HV monomer.

In tissue engineering, the mean approach is to mimic the natural extracellular matrix (ECM). The ECM plays an important role in regulating cellular behaviors. It has two main components polysaccharides and fibrous proteins. Therefore, nanofibrous structures have been used as tissue engineering platforms (Liang et al. 2007). We used the method of electrospining to form aligned nanofiber scaffold. Electrospinning is a method of producing continuous micro-nanofiber. Electrospinning parameters such as polymer solution concentration, viscosity, collector distance, and electrical field strength may be varied to form different architecture and morphology of the scaffold. We optimized the electrospinning parameters as 5% PHBV concentration (w/v), 20kV applied potential, and 3100 rpm drum collector speed. For neural tissue engineering, electrospun nanofibrous scaffolds have been investigated by several research groups both in vivo and in vitro. Axonal extensions within electrospun fibrous nerve conduits and partial functional reconnection have been demonstrated (Panseri et al. 2008). In tissue engineering for nerve repair, the ability to enhance axon extension is an essential factor (Johansson et al. 2006). Electrospun scaffolds with aligned nanofibers are gaining importance in providing topographical cues for nerve regeneration. There are many studies in the literature that neurons cultured on aligned electrospun fibers have longer dendrite lengths than those on random fibers (Chow et al. 2007). That is why we use aligned nanofiber scaffold as nerve conduit for peripheral nerve regeneration in this study.

Mechanical property of a scaffold material is an important aspect. The scaffold must be capable of forming a mechanical integrity to repair an injury. Hence, mechanical properties of the aligned PHBV scaffold were determined. The mean value and standard deviation found for tensile strength was 18.33 ± 1.32 N/mm^2; elongation at break was $19.33 \pm 0.4\%$, and E modulus was 195.26 ± 13.98 N/mm^2. Recently, it was found that randomly organized electrospun PHBV nanofibers and their scaffolds have lower mechanical properties than their aligned counterparts (Purushothaman et al. 2011). But, Kwon and his colleagues found that Young's modulus of the randomly organized electrospun PHBV nanofiber scaffolds was 350 ± 30, tensile strength was 8.6 ± 0.8 and elongation at break was 19.5 ± 1.5 (Oh et al. 2007). Tong and Wang determined that tensile strength and Young's modulus of aligned PHBV nanofiber scaffolds were

greater than randomly organized nanofiber scaffolds and also fiber orientation did not play a significant role in affecting the elongation at break, but the fiber diameter did (Ho and Min 2006).

PHBV nanofibrous scaffold was formed into tube shape by suturing through the alignment axis. It was observed that, PHBV tube was stable. It is an advantage of PHBV nanofiber conduit that it does not involve any chemical reactions during PHBV tube forming. In a nerve gap, failure of axons to regenerate, reaching of the regenerated axons to the distal stump too late, or the number of axons reaching the distal stump to be too few, can cause problem for functional recovery. Therefore, for manipulation of the local environment, aligned bacterial PHBV nanofiber conduit was formed and used to repair nerve gap. The physical characteristic of aligned PHBV nanofiber scaffold is suitable to use as a peripheral nerve conduit (Yiqian et al. 2011).

In the study, PHBV graft-guided regeneration was compared with autografting, which is the gold standard. For peripheral nerve repair, functional organ re-innervation is the main issue. Therefore, axonal regeneration was assessed by walking analysis (Vleggeert-Lankamp 2007) and electrophysiological assessment (Wolthers et al. 2005). Obtained CMAP % and SFI values mean that axonal regeneration was occurred for all rats of PHBV group. Both walking and electrophysiology analyses showed that axonal regeneration was occurred throughout the PHBV conduit, but it was lower than that of the autograft group (Figures 4 and 5). In this point, major limitation is the slower growth of nerve fibers and relatively poor re-innervation of target muscle. It should be noted that, atrophy was observed in all rats. These results indicate that aligned PHBV nanofibrous conduit has long-term effects on nerve regeneration, and the *in vivo* performance of the PHBV conduit is parallel to that of the autografts.

At the 8th and 16th weeks after the operations, on microscopic examinations, it was seen that PHBV graft was minimally degraded *in vivo*. Agarose-based scaffolds were used for nerve repair studies in the literature. In this study, PHBV grafts were filled with agarose. At the end of the 8th and 16th weeks, no collapsed graft was noted (Mahesh and Ravi 2008).

Histological assessment was used to determine the axon number and the diameter of the myelin thickness on the regenerating axons in both groups, at the 8th and 16th weeks after the operation. (Evans et al. 1999, Jason et al. 2005). PHBV graft group contained more blood vessels compared to autograft group on Week 8, which should help regeneration by delivering the nutrients to the operated nerve (Young et al. 2002). The surfaces of the PHBV graft exhibited a capsule consisting of mononuclear phagocytic cells, giant cells, lymphocytes, and fibroblasts, which could be easily removed. This tissue reaction did not differ statistically between the two time periods (Mohanna et al. 2003). In the autograft group, a well-coordinated and healthy regenerating nerve exhibiting regular fascicles of axons was noted. The nerve myelin sheaths and the vascular elements were very well defined in this group (Mahesh and Ravi 2008). The number of axons was significantly higher in autograft group when compared to those of the PHBV graft group at the end of the 8th and 16th weeks. No significant difference was observed between the PHBV graft group related to the number of the axons and the blood vessels on Week 16. At the transmission electron microscopic level, all groups exhibited varying amounts of myelinating single or clustered nerve fibers surrounded by schwann cells (Mohanna et al. 2005). The myelin sheath thickness was not statistically different in autograft group when compared to the PHBV graft group. As a conclusion, the PHBV tube application slightly improved the nerve regeneration process compared to the control on Week 16 (Hazari et al. 1999).

Conclusion

As a conclusion, this study demonstrates that *A. eutrophus* (DSM 545) accumulate PHBV copolymer, when supplied with 10g/L glucose and 20g/L propionic acid. Aligned PHBV scaffold is easily formed by electrospinning technique and can be shaped as a nerve conduit. Aligned PHBV scaffold permitted peripheral nerve regeneration after experimental sciatic nerve injury. This regeneration is comparable with autografting, although regeneration seemed better and quicker with autografting. In our opinion, these results indicate that PHBV may be a useful conduit for nerve gap repair. Axonal regeneration in a PHBV graft may be further improved, to obtain optimal nerve regeneration by some modifications in the future studies.

Acknowledgement

The authors would like to thank Cengiz Uzun and Ahmet Çabuk for characterization of PHBV, Cem Bayram, Özgür Demirbilek and Melike Erol Demirbilek for the preparation of this paper.

Declaration of interest

The authors report no declarations of interest. The authors alone are responsible for the content and writing of the paper.

References

Anil Kumar PK, Shamala TR, Kshama L, Prakash MH, Joshi GJ, Chandrashekar A, et al. 2007. Bacterial synthesis of poly (hydroxybutyrate-co-hydroxyvalerate) using carbohydrate-rich mahua (Madhuca sp.) flowers. J Appl Microbiol. 103:204–209.

Baki H. 2010. Amphiphilic Poly (3-hydroxyalkanoate)s: potential candidates for medical applications. Int J Polym Sci. Article ID 423460. doi:10.1155/2010/423460.

Bolgen N, Vargel I, Korkusuz P, Menceloğlu YZ, Pişkin E. 2007. In vivo performance of antibiotic embedded electrospun PCL membranes for prevention of abdominal adhesions. J Biomed Mat Res Part B Appl Biomater. 81B:530–543.

Chamberlain LJ, Yannas IV, Arrizabalaga A, Hsu HP, Norregaard TV, Spector M. 1998. Early peripheral nerve healing in collagen and silicone tube implants: Myofibroblasts and the cellular response. Biomaterials. 19:1393–1403.

Chen YS, Hu CL, Hsieh CL, Lin JG, Tsai CC, Chen TH, Yao CH. 2001. Effects of percutaneous electrical stimulation on peripheral nerve regeneration using silicone rubber chambers. J Biomed Mater Res. 57:541–549.

Chew BSY, Mi R, Hoke A, Leong KW. 2007. Aligned protein–polymer composite fibers enhance nerve regeneration: a potential tissue-engineering platform. Adv Funct Mater. 17:288–1296.

Chow WN, Simpson DG, Bigbee JW, Colello RJ. 2007. Evaluating neuronal and glial growth on electrospun polarized matrices: bridging the gap in percussive spinal cord injuries. Neuron Glia Biol. 3:119–126.

Chun JC, Yen CO, Su LL, Wen YC, Shih YC, Ching WW, et al. 2007. Transplantation of bone marrow stromal cells for peripheral nerve repair. Exp Neurol. 204:443–453.

Dodla MC, Bellamkonda RV. 2008. Differences between the effect of anisotropic and isotropic laminin and nerve growth factor presenting scaffolds on nerve regeneration across long peripheral nerve gaps. Biomaterials. 29:33–46.

Evans GR, Brandt K, Widmer MS, Lu L, Meszlenyi RK, Gupta PK, et al. 1999. In vivo evaluation of poly(L-lactic acid) porous conduits for peripheral nerve regeneration. Biomaterials. 20:1109–1115.

Gaudio CD, Fioravanzo L, Folin M, Marchi F, Ercolani E, Bianco A. 2012. Electrospun tubular scaffolds: on the effectiveness of blending poly(ε-caprolactone) with poly(3-hydroxybutyrate- co-3-hydroxyvalerate). J Biomed Mater Res Part B Appl Biomater. 100B:1883–1898.

Hazari A, Wiberg M, Johansson GR, Green C, Terenghi G. 1999. A resorbable nerve conduit as an alternative to nerve autograft in nerve gap repair. Br J Plast Surg. 52:653–657.

Ho WT, Min W. 2006. Electrospinning of fibrous PHBV tissue engineering scaffolds: fiber diameter control, fiber alignment and mechanical properties. Proceedings of the Biomedical Engineering Conference (BME) Hong Kong, 21–23 September 2006, p. 55–58.

Jain A, Kim YT, McKeon RJ, Bellamkonda RV. 2006. In situ gelling hydrogels for conformal repair of spinal cord defects, local delivery of BDNF after spinal cord injury. Biomaterials. 27:497–504.

Jason SB, Catherine AM, Molly SS, Rajiv M. 2005. Peripheral nerve regeneration through a synthetic hydrogel nerve tube. Restor Neurol Neurosci 23:19–29.

Jian T, Cunjiang S, Mingfeng C, Dan H, Li L, Na L, Shufang W. 2009. Thermal properties and degradability of poly (propylene carbonate)/poly (β-hydroxybutyrate-co-β-hydroxyvalerate) (PPC/PHBV) blends. Polym Degrad Stab. 94:575–583.

Johansson F, Carlberg P, Danielsen N, Montelius L, Kanje M. 2006. Axonal outgrowth on nanoimprinted patterns. Biomaterials. 27:1251–1258.

Kiyotani T, Nakamura T, Shimizu Y, Endo K. 1995. Experimental study of nerve regeneration in a biodegradable tube made from collagen and poly glycolic acid. Asaio J. 41:M657–661.

Koh HC, Park JS, Jeong MA, Hwang HY, Hong YT, Ha SY, Nam SY. 2008. Preparation and gas permeation properties of biodegradable polymer/layered silicate nanocomposite membranes. Desalination. 233:201–209.

Liang D, Hsiao BS, Chu B. 2007. Functional electrospun nanofibrous scaffolds for biomedical applications. Adv Drug Deliv Rev. 59: 1392–1412.

Linko S, Vaheri HJS. 1993. Production poly-β-hydroxybutyrate on lactic acid by *Alcaligenes eutrophus* H16 in a 3-1 bioreactor. Enzyme Microb Technol. 15:401–406.

Longan S, Seong CY, Hyun GP, Ho NC. 2004. Sequential feeding of glucose and valerate in a fed-batch culture of ralstonia eutropha for production of poly (hydroxybutyrate-co-hydroxyvalerate) with high 3-hydroxyvalerate fraction. Biotechnol Prog. 20:140–144.

Mahesh CD, Ravi VB. 2008. Differences between the effect of anisotropic and isotropic laminin and nerve growth factor presenting scaffolds on nerve regeneration across long peripheral nerve gaps. Biomaterials. 29:33–46.

Mahuya M, Patra A, Paul AK. 2005. Production of poly (3-hydroxybutyrate) and poly (3-hydroxybutyrate-co-3-hydroxyvalerate) by *Rhodopseudomonas palustris* SP5212. World J Microbiol Biotechnol. 21:765–769.

Matsumoto K, Kitagawa K, Jo SJ, Song Y, Taguchi S. 2011. Production of poly (3-hydroxybutyrate-co-3-hydroxyvalerate) in recombinant *Corynebacterium glutamicum* using propionate as a precursor. J Biotechnol. 152:144–146.

Mligiliche N, Endo K, Okamoto K, Fujimoto E, Ide C. 2001. Extracellular matrix of human amnion manufactured into tubes as conduits for peripheral nerve regeneration. J Biomed Mater Res (Appl Biomater). 63:591–600.

Mohanna PN, Young RC, Wiberg M, Terenghi GA. 2003. A composite poly hydroxybutyrate glial growth factor conduit for long nerve gap repairs. J Anat. 203:553–565.

Noble J, Munro CA, Prasad VS, Midha R. 1998. Analysis of upper and lower extremity peripheral nerve injuries in a population of patients with multiple injuries. J Trauma. 45:116–122.

Oh HK, Ik SL, Young GK, Wan M, Kyung HJ, Inn KK, Yoshihiro I. 2007. Electrospinning of microbial polyester for cell culture. Biomed Mater. 2:52–58.

Ozkan M, Gokmen N, Yilmaz O, Erbayraktar S, Bagriyanik A. 2010. Effect of erythropoietin on peripheral nerve regeneration. J Neurol Sci Turk. 27:035–042.

Panseri S, Cunha C, Lowery J, Carro UD, Taraballi F, Amadio S, Vescovi AF. 2008. Gelain, electrospun micro and nano fiber tubes for functional nervous regeneration in sciatic nerve transections. BMC Biotech. 8–39.

Mohanna PN, Terenghi G, Wiberg M. 2005. Composite PHB-GGF conduit for long nerve gap repair: a long-term evaluation. Scand J Plast Reconstr Surg Hand Surg. 39:129–137.

Purushothaman K, Kirthanashri SV, Dhakshinamoorthy S, Uma MK, Swaminathan S. 2011. Development of poly (3-hydroxybutyrate-co-3-hydroxyvalerate) fibers for skin tissue engineering: effects of topography, mechanical, and chemical stimuli. Biomacromolecules. 12:3156–3165.

Ren Q, Sierro N, Kellerhals M, Kessler B, Witholt B. 2000. Properties of engineered poly-3-hydroxyalkanoates produced in recombinant *Escherichia coli* strains. Appl Environ Microbiol. 66:1311–1320.

Stevenson TR, Kadhiresan VA, Faulkner JA. 1994. Tubular nerve guide and epineurial repair: comparison of techniques for neurorrhaphy. J Reconstr Microsurg. 10:171–174.

Susheela BG. 2012. Spectroscopic estimations of composition of engineered polyphenylene oxide copolymers. Int J Eng Res Dev. 1:80–83.

Trumble TE, Shon FG. 2000. The physiology of nerve transplantation. Hand Clin. 16:105–122.

Valentini RF, Sabatini AM, Dario P, Aebischer P. 1989. Polymer electret guidance channels enhance peripheral nerve regeneration in mice. Brain Res. 480:300–304.

Vleggeert-Lankamp CL. 2007. The role of evaluation methods in the assessment of peripheral nerve regeneration through synthetic conduits: a systematic review. Laboratory investigation. J Neurosurg. 107:1168–1189.

Wang J, Yu J. 2001. Kinetic analysis on formation of poly (3-hydroxybutyrate) from acetic acid by *Ralstonia eutropha* under chemically defined conditions. J Ind Microbiol Biotechnol. 26:121–126.

Wolthers M, Moldovan M, Binderup T, Schmalbruch H, Krarup C. 2005. Comparative electrophysiological, functional and histological studies of nerve lesions in rats. Microsurgery. 25:508–519.

Yiqian Z, Aijun W, Shyam PI, Kyle K, Edward D, Xuan B, et al. 2011. Engineering Bi-layer nanofibrous conduits for peripheral nerve regeneration. Tissue Eng Part C 17:7.

Yoon JC, Hyung JC, Jo SY, Young JY. 1997. Production of poly (3-Hydroxybutyric-co-3-Hydroxyvaleric) acid using propionic acid by pH regulation. J Ferment Bioeng. 83:492–495.

Young RC, Wiberg M, Terenghi G. 2002. Poly-3-hydroxybutyrate (PHB): a resorbable conduit for long-gap repair in peripheral nerves. Br J Plast Surg. 55:235–240.

Yu X, Bellamkonda RV. 2003. Tissue-engineered scaffolds are effective alternatives to otografts for bridging peripheral nerve gaps. Tissue Eng. 9:421–430.

Zhao L, He C, Gao Y, Cen L, Cui L, Cao Y. 2008. Preparation and cytocompatibility of PLGA scaffolds with controllable fiber morphology and diameter using electrospinning method. J Biomed Mater Res Part B Appl Biomater. 87B:26–34.